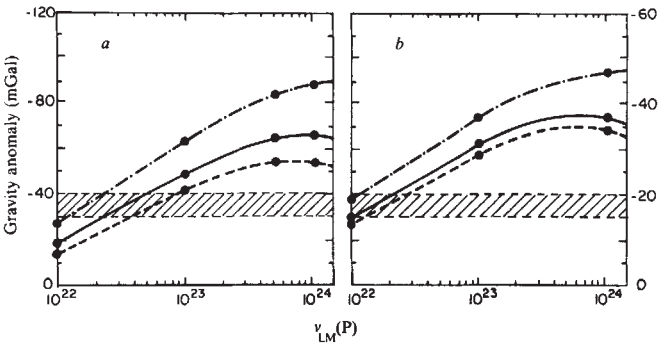

Fig. 4 Predicted present-day peak free air gravity anomaly at the centre of disk model Laurentian (*a*) and Fennoscandian (*b*) loads as a function of the viscosity of the mantle beneath 670 km depth. The viscosity of the upper mantle is held fixed at 10^{22} P. The hatched region on each plate denotes the observed peak anomaly in the corresponding region.

which have lower mantle viscosities of 10^{22} P and 10^{23} P respectively and upper mantle values of 10^{22} P. The solid curves are based on the assumption of isostatic equilibrium while the dashed curves include the influence of a load history constrained by $^{18}O/^{16}O$ data from deep sea sedimentary cores[8]. Since all the data are bracketed by the predictions of L1 and L2 the implication is that lower mantle viscosity ν_{LM} is such that $10^{22}\,P \leq \nu_{LM} \leq 10^{23}$ P. These sea level data therefore exclude the higher of the two values of ν_{LM} allowed by the $\dot{J}_2$ observation and from Fig. 1 we have

$$2.7\times10^{22}\quad P \leq \nu_{LM}\,(\text{Lageos}) \leq 4.4\times10^{22}\quad P \qquad (7)$$

One further piece of observational evidence which may be used to confirm equation (7) consists of surface free air gravity anomalies over the main centres of Pleistocene deglaciation. Figure 3 shows free air gravity maps for Hudson Bay and the Gulf of Bothnia. The peak free air anomaly over the former region is near −40 mGal whereas that over the latter, appropriately corrected for large-scale bias, is near −17 mGal (ref. 8). These observed peak anomalies are shown as the cross-hatched regions on Fig. 4 where they are compared with theoretical predictions of models which differ from one another only in their values of ν_{LM}. Focusing attention on the solid lines on each plate, which are the most accurate predictions[12,13], we note that the value of the lower mantle viscosity required by the free air gravity data is in accord with that inferred from the new $\dot{J}_2$ observation.

The fact that the ν_{LM} inferred from Lageos tracking data agrees with that required by local gravity anomalies suggests that the viscosity of the lower mantle may not have appreciable large-scale heterogeneity. This is expected if this region of the Earth is well mixed by convection. Also, the observed increase of the viscosity across the seismic discontinuity at 670 km depth is most easily understood if the temperature change at this depth is adiabatic[14]. This situation will hold only if the circulation is whole mantle in scale and mass transport through the 670-km phase boundary is unimpeded.

Unfortunately, this argument for whole mantle convection is not definitive. We are not yet able to exclude the possibility of a layered convective circulation with a sharp thermal boundary layer at 670 km depth. In this scenario, the rapid increase of temperature through the boundary layer would have to be accompanied by a rather large increase of creep activation energy[14] in order that the viscosity of the lower mantle remain near the viscosity of the upper mantle as required by the new $\dot{J}_2$ observation. This model has the additional interesting feature that there would exist a thin layer of very low viscosity at the base of the upper mantle on the spinel side of the 670-km phase transformation. Work is in progress to determine whether the presence of such a layer can be ruled out on the basis of the relative sea level, free air gravity, and rotation data of postglacial rebound. The new $\dot{J}_2$ observation from Lageos laser ranging data is an important addition to the data set which we are using in a study of the inverse problem for the viscosity of the Earth's mantle.

Received 25 February; accepted 13 June 1983.

1. Yagi, T., Bell, P. M. & Mao, H. K. *Yb Carneqie Instn Wash.* **78,** 614–618 (1979).
2. Richter, F. M. *Geophys. J. R. astr. Soc.* **35,** 365–376 (1973).
3. Rubincam, D. P. in *Abstr. 5th A. NASA Geodynamics Program Conf. and Crustal Dymamics Project Review,* 31 (NASA Headquarters, Washington DC, 1983).
4. Yoder, C. F. *et al. Nature* **303,** 757–762 (1983).
5. Kaula, W. M. *Theory of Satellite Geodesy* (Blaisdell, Massachussetts, 1966).
6. Lambeck, K. *The Earth's Variable Rotation: Geophysical Causes and Consequences* (Cambridge University Press, London, 1980).
7. Dicke, R. H., in *The Earth–Moon System* (eds Marsden, B. G. & Camero, A. G. W.) (Plenum, New York, 1966).
8. Peltier, W. R. *Adv. Geophys.* **24,** 1–146 (1982).
9. O'Connell, R. J. *Geophys. J. R. astr. Soc.* **23,** 299–327 (1971).
10. Nakiboglu, S. M. & Lambeck, K. *Geophys. J. R. astr. Soc.* **62,** 49–58 (1980).
11. Sabadini, R. & Peltier, W. R. *Geophys. J. R. astr. Soc.* **66,** 533–578 (1981).
12. Wu, P. & Peltier, W. R. *Geophys. J. R. astr. Soc.* **72,** (in the press).
13. Peltier, W. R. & Wu, P. *Geophys. Res. Lett.* **9,** 731–734 (1982).
14. Peltier, W. R. & Jarvis, G. T. *Phys. Earth planet. Inter.* **29,** 281–304 (1982).

Visual motion and cortical velocity

A. Johnston & M. J. Wright

Department of Psychology, Brunel University, Kingston Lane, Uxbridge, Middlesex UB8 3PH, UK

Recent studies have revealed some remarkably simple relationships between visual performance and the neuroanatomy of the visual pathways. The visual field is mapped topographically on the surface of the striate cortex in man; the projection is large for the central visual field and is progressively compressed towards the periphery. Visual acuity decreases with distance from the fovea in proportion to the estimated cortical magnification factor, *M* (the extent of striate cortex in millimetres corresponding to a degree of arc in visual space)[1]. If a stimulus is magnified at peripheral locations in proportion to 1/*M*, it becomes equally resolvable across the visual field[2–5]. This scaling procedure (*M*-scaling) maintains equivalence of the cortical projection of stimuli with different visual field loci. We have used *M*-scaling to investigate motion perception as a visual field variable. We report here that both the lower threshold of motion and adaptation to motion are uniform for *M*-scaled stimuli, and are related to the velocity of the 'cortical image'.

The sensitivity to contrast (1/threshold contrast) of the human visual system is usually determined as a function of the spatial frequency (cycles per degree of visual angle) of grating patterns with sine-wave luminance profiles. Contrast sensitivity decreases in a systematic manner as gratings are positioned further into the periphery of the visual field. *M*-scaling increases the angular subtense and reduces the spatial frequency of grating patches having increasing visual field eccentricity while maintaining constant their cortical spatial frequency (cycles mm^{-1}). Contrast sensitivity functions measured using *M*-scaled gratings at different positions in the visual field superimpose when plotted in terms of cortical spatial frequency[2–5]. These relationships are independent of the rate of flicker or drift of the grating[4,6] and also apply to colour contrast[5]. *M*-scaling shows the contrast sensitivity of central and peripheral visual fields to be quantitatively rather than qualitatively different. Qualitative differences may, however, exist when we consider other metrics of visual function, such as vernier acuity[7].

There have been several recent reports that moving patterns viewed in the periphery can be seen to slow down or stop[8–12], suggesting major differences in motion thresholds for foveal and peripheral vision which might be explicable in terms of the cortical magnification factor. We decided to investigate this phenomenon, quantifying the rate of movement at which a drifting grating can just be distinguished from a stationary one

0028–0836/83/310436—03$01.00

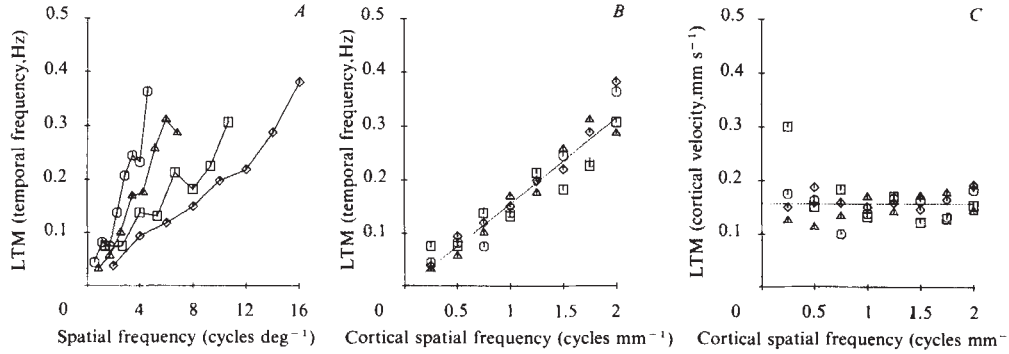

Fig. 1 *A*, The lower threshold of motion (LTM) expressed as temporal frequency (ordinate) for gratings of various spatial frequencies (abscissa) measured at four eccentricities: ◇, 0 deg; □, 1.5 deg; △, 4 deg; ○, 7.5 deg. *B*, The abscissa has been transformed to provide values in terms of cortical spatial frequency. Regression line fitted by least-squares method. *C*, The ordinate has also been transformed to express the LTM in terms of cortical velocity. Subject A.J.

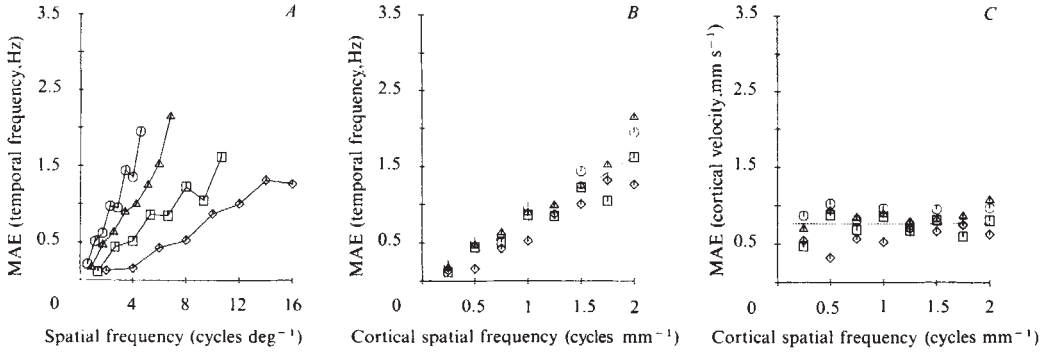

Fig. 2 *A*, Motion aftereffect (MAE) expressed as temporal frequency (ordinate) for gratings of various spatial frequencies (abscissa) measured at four eccentricities: ◇, 0 deg; □, 1.5 deg; △, 4 deg; ○, 7.5 deg. Adapt and test spatial frequencies were always the same. *B*, The abscissa has been transformed to provide values in terms of cortical spatial frequency. Regression line fitted by least-squares method. *C*, The ordinate has also been transformed to express the MAE in terms of cortical velocity. Subject M.J.W.

(lower threshold of motion) as a function of spatial frequency at four eccentricities.

A vertical sinusoidal grating was viewed binocularly through a semi-circular aperture in a mask of the same mean luminance (100 cd m^{-2}) at a distance of 200 cm (ref. 6). The aperture had a horizontal base of 7 cm and the grating was fixated at the centre of the base for foveal viewing, or using a series of fixation ots placed vertically below for eccentric viewing. To maintain a constant state of contrast adaptation, a stationary grating (contrast 0.3) was inspected for 30 s at the start of each trial. Following this there were one 6-s and five 4-s periods during which the observer could control the drift rate of this grating by the adjustment of a multi-turn potentiometer. The rate of drift was increased until movement of the grating could just be discerned. Intervals during which adjustments could be made were interspersed with 3-s periods in which a stationary grating was re-instated. A subsequent control experiment using a blank screen of average mean luminance instead of the stationary grating gave similar results. Settings were obtained for 8 spatial frequencies ($SF = 2$, 4, 6, 8, 10, 12, 14 and 16 cycles deg^{-1}) and each data point is an average of thresholds determined for just discernible movement in each of the two horizontal directions of drift. These observations were repeated in identical conditions but with fixation displaced along the lower vertical meridian and viewing distance altered in accordance with *M*-scaling. Thus, there were four sets of measurements with fixation points 0, 3.5, 6 and 7.5 cm and corresponding viewing distances of 200, 133, 86 and 57 cm so that the lower edge of the aperture fell 0, 1.5, 4 and 7.5 deg from the fixation points. This ensured that each spatial frequency presented decreased with eccentricity such that SF/M (cortical spatial frequency) remained constant. Values of M for these eccentricities have been taken from Virsu *et al.*[4].

We plotted the magnitude of the lower threshold of motion (LTM) against spatial frequency (Fig. 1*A*) and cortical spatial frequency (Fig. 1*B*) for subject A.J. (The results for M.J.W. were in close correspondence.) LTM, expressed as temporal frequency (number of grating cycles passing a fixed point per second, Hz), increased in an approximately linear fashion with spatial frequency for all eccentricities studied. As velocity = temporal frequency/spatial frequency, we may infer from the data of Fig. 1*A* that LTM at a given visual field locus approximates to a constant velocity for all spatial frequencies. These data complement the finding[13] that the threshold for detecting an instantaneous displacement (IDT) for a centrally fixated grating is a constant distance for all spatial frequencies. LTM velocity and IDT are thus both independent of spatial frequency. The LTM measured as a retinal variable increases with eccentric viewing, as expected (Fig. 1*A*). When scaled with respect to the cortical magnification factor, differences in the slopes of these functions disappeared (Fig. 1*B*). Figure 1*C* demonstrates that the LTM is constant in terms of cortical velocity: the average value for A.J. was 0.16 mm s^{-1} and for M.J.W. 0.15 mm s^{-1}. For comparison, Cowey and Rolls[14] found the minimum angle of resolution to be equivalent to a cortical distance of 0.084 mm.

LTM is independent of spatial frequency. Generally, for cells in retina[15] and cortex[16], the optimal spatial frequency is inversely related to receptive field size, therefore the size of receptive fields in retina or cortex does not determine LTM. The increase in LTM considered as a retinal variable correlates with the decrease in cell density with eccentricity found in the retino-cortical mapping[1], but LTM is most economically described as a constant threshold cortical translation velocity.

Barlow[17] has proposed a mechanism whereby spatiotemporal resolution would depend on cell density in the cortex. He argues that cells in the striate cortex can improve on the spatial resolution of retinal ganglion cells by a process of interpolation. Cortical cells would form graded links to groups of input fibres to define the interpolation function. The velocity resolution of striate cortex would also depend on cortical cell density. Assuming uniform cell density across the striate cortex[18] and assuming temporal homogeneity[4,6], the velocity resolution of the visual field would vary according to the cortical magnification factor.

Constant cortical velocity thresholds provide a partial explanation of the phenomenon of stopped visual motion. As a grating of a given spatial frequency is moved further into the periphery the cortical image will decrease in size. Eventually, the visual cortex will not be able to resolve small cortical translations within the temporal constraints of the velocity mechanism.

Following prolonged inspection of a pattern moving in a given direction, a stationary pattern will appear to move in the opposite direction. This illusion is the motion aftereffect, MAE (Thompson[19] provides a recent review). In a previous experiment we noted the slowing of gratings when viewed in the

periphery. We thought that greater adaptation to motion in the periphery might add to the stopped motion effect. The MAE was quantified as the temporal frequency of drift required to cancel the illusory perception of motion. Provided fixation was steady, an unambiguous, coherent percept was available at all times and cancellation gave a convincing perception of a steady grating. We adapted for 60 s to a grating (contrast 0.3) drifting at 8 Hz and allowed one 3-s and five 2-s periods in which control over drift rate was passed to the observer, to achieve cancellation of the aftereffect. These adjustment periods were interspersed with 6 s of top-up adaptation. Otherwise, the same experimental conditions were used for MAE as for the LTM determination. Figure 2*A–C* shows data for M.J.W. (each data point is the average of the MAE in both directions of drift). The MAE measured in terms of cortical velocity was on average 0.78 mm s^{-1} for M.J.W. and 1.2 mm s^{-1} for A.J. This value was constant within the limits of measurement error for different spatial frequencies and eccentricities, but would be influenced by adaptation time and test interval as well as inter-subject differences. We find the velocities of the MAE to be much greater than the LTM (note the different ordinates for Figs 1 and 2).

There is an interesting paradox in the data. The temporal frequency of the adapt grating was constant, thus its velocity decreased with increasing spatial frequency. Although the velocity of the adapt grating was variable, the velocity of the aftereffect was constant at a given retinal eccentricity and its cortical velocity was constant for all measurements. This may underlie difficulties in determining whether the coding process in motion perception is based on temporal frequency or velocity.

The *M*-scaled properties of the LTM and MAE provide evidence that in the analysis of visual motion, the near periphery is not qualitatively different from foveal vision. The slowing up of peripherally viewed stimuli and the stopped motion effect may be explained by reference to the velocity of the cortical representation.

We thank the MRC for support (grant no. G979/1106/N).

Received 27 April; accepted 22 June 1983.

1. Drasdo, N. *Nature* **226,** 554–556 (1977).
2. Rovamo, J., Virsu, V. & Nasanen, R. *Nature* **271,** 54–56 (1978).
3. Virsu, V. & Rovamo, J. *Expl Brain Res.* **37,** 475–494 (1979).
4. Virsu, V., Rovamo, J., Laurinen, P. & Nasanen, R. *Vision Res.* **22,** 1211–1217 (1982).
5. Noorlander, C., Koenderink, J. J., den Ouden, R. J. & Edens, B. W. *Vision Res.* **23,** 1–11 (1983).
6. Wright, M. J. & Johnston, A. *Vision Res.* (in the press).
7. Westheimer, G. *Vision Res.* **22,** 157–162 (1982).
8. Lichtenstein, M. *J. opt. Soc. Am.* **53,** 302–306 (1963).
9. Campbell, F. W. & Maffei, L. *Nature* **278,** 192 (1979).
10. Campbell, F. W. & Maffei, L. *Vision Res.* **21,** 713–721 (1981).
11. MacKay, D. M. *Perception* **11,** 359–360 (1982).
12. Tynan, P. D. & Sekuler, R. *Vision Res.* **22,** 61–68 (1982).
13. Westheimer, G. *Vision Res.* **18,** 1073–1074 (1978).
14. Cowey, A. & Rolls, E. T. *Expl Brain Res.* **21,** 447–454 (1974).
15. Enroth-Cugell, C. & Robson, J. G. *J. Physiol., Lond.* **187,** 517–552 (1976).
16. Kulikowski, J. J. & Vidyasagar, T. R. *J. Physiol., Lond.* **332,** 10–11P (1982).
17. Barlow, H. B. *Proc. R. Soc.* **B212,** 1–34 (1981).
18. Hubel, D. H. & Wiesel, T. N. *Proc. R. Soc.* **B198,** 1–59 (1977).
19. Thompson, P. thesis, Univ. Cambridge (1976).

A functional role for vasoactive intestinal polypeptide in anterior cingulate cortex

James McCulloch & Paul A. T. Kelly

Wellcome Surgical Institute, University of Glasgow, Glasgow G61 1QH, UK

Vasoactive intestinal polypeptide (VIP) is present in high concentrations in the cerebral cortex, where it is the putative neurotransmitter of a major intracortical neuronal system[1–3]. Homogenates of cortical tissue contain high-affinity, specific binding sites for VIP[4] as well as an adenylate cyclase system which is sensitive to this peptide[5,6]. As with many of the other peptidergic systems which have been identified in the central nervous system (CNS), it has proved extremely difficult to elucidate the nature and extent of the functional role of VIP in specific brain areas. Here, using the quantitative autoradiographic ^{14}C-deoxyglucose technique in rats[7] to provide insight into functional processes[8], we describe the increases in glucose utilization which occur locally in anterior cingulate cortex following the unilateral injection of VIP (20 pmol) into this key brain area and, additionally, the focal alterations in glucose use in CNS regions having known neuronal connections with the injected region (for example, ipsilateral mediodorsal thalamus, ventral tegmental area, nucleus accumbens, caudate nucleus and contralateral cingulate cortex). These data provide evidence that VIP may modify the processing of afferent and efferent information within the anterior cingulate cortex in the conscious rat.

The effects of intracingulate injections of artificial cerebrospinal fluid (CSF) or VIP (20 pmol) on local cerebral glucose phosphorylation in 31 anatomically discrete regions of the CNS are shown in Table 1. VIP increased glucose utilization in the anterior cingulate cortex and in several CNS regions having known neuronal connections with the injection site[9], the most notable being in the contralateral anterior cingulate cortex, nucleus accumbens, ventral tegmental areas and mediodorsal thalamic nuclei of both hemispheres (Table 1, Fig. 1). Reduced glucose utilization was observed following intracortical VIP administration only in that portion of the caudate nucleus (the dorsomedial aspect) (Fig. 2) to which the major fraction of striatal afferents from anterior cingulate cortex are directed[9]. In contrast, glucose use elsewhere in the caudate nucleus was unaltered by the intracortical neuropeptide administration. We emphasize that rates of glucose utilization were similar following cortical injections of VIP or CSF in the overwhelming majority of cerebral areas examined, including several regions having direct neuronal connections with the anterior cingulate cortex (for example, anterior thalamus, amygdala; Table 1). These differential effects of cortical VIP mechanisms in altering activity in only some of the neuronal circuits routed through the anterior cingulate cortex provide further support for a subtle, physiological role for VIP.

Dynamic alterations in glucose utilization seem to reflect predominantly activity in axonal terminals of neuronal pathways[10]; and, thus, measurements of focal changes in glucose can be used to identify neuroanatomical circuits which are being activated[8]. The distribution of the alterations of glucose utiliz-

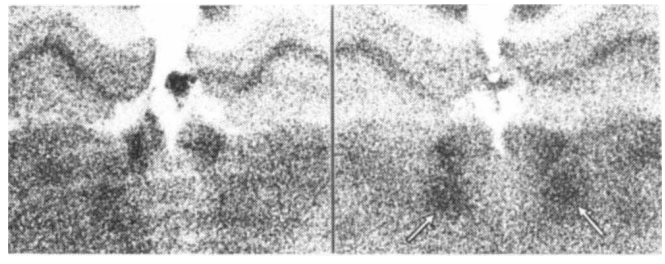

Fig. 1 Representative 2-deoxyglucose autoradiograms at the level of the mediodorsal thalamic nucleus within each animal. Relative rates of glucose utilization are related directly to relative optical density. Following intracingulate injection of CSF (left), glucose use in the mediodorsal thalamic nuclei is similar to that of adjacent thalamic areas and lower than that in the lateral habenular nucleus of the epithalamus. Following cingulate injections of VIP (20 pmol) (right), glucose use in the mediodorsal thalamic nuclei (arrowed) is greater than that of adjacent thalamic areas and similar to that in the lateral habenular nuclei.

0028–0836/83/310438—03$01.00